HHS Public Access

Author manuscript

Front Neuroendocrinol. Author manuscript; available in PMC 2017 January 01.

Published in final edited form as:

Front Neuroendocrinol. 2016 January ; 40: 42–51. doi:10.1016/j.yfrne.2015.10.001.

In vivo visualization of aromatase in animals and humans

Anat Biegon

Dept. Neurology, Stony Brook University School of Medicine

Abstract

Aromatase catalyzes the last and obligatory step in the biosynthesis of estrogens across species. In vivo visualization of aromatase can be performed using positron emission tomography (PET) with radiolabeled aromatase inhibitors such as [^{11}C]vorozole. PET studies in rats, monkeys and healthy human subjects demonstrate widespread but heterogeneous aromatase availability in brain and body, which appears to be regulated in a species, sex and region-specific manner. Thus, aromatase availability is high in brain amygdala and in ovaries of all species examined to date, with males demonstrating higher levels than females in all comparable organs. However, the highest concentrations of aromatase in the human brain are found in specific nuclei of the thalamus while the highest levels in rats and monkeys are found in the amygdala. Regional brain aromatase availability is increased by androgens and inhibited by nicotine. Future studies may improve diagnosis and treatment in brain disorders and cancers overexpressing aromatase.

Keywords

Positron emission tomography; PET; vorozole; aromatase inhibitors

1. Introduction

Gene expression and enzyme activity studies have established that aromatase is present in most peripheral organs as well as in the brain of both mammalian and non-mammalian species including fish, birds, rodents, non-human primates and humans (Naftolin et al., 1996, Reviewed in Simpson et al., 2002). In vivo visualization of aromatase only became possible following the development and validation of specific radiopharmaceuticals which, in conjunction with positron emission tomography (PET), could be used to produce three dimensional, quantitative maps of aromatase availability throughout the body. This step was facilitated by the discovery and clinical development of potent and specific drugs designed to inhibit aromatase (aromatase inhibitors, AI), which are increasingly replacing estrogen receptor antagonists in the hormonal treatment of breast cancer (Bonneterre et al., 2000; Budzar and Howell, 2001; Cohen et al., 2002, Howell et al., 2005) with potential use in

Corresponding Author: Anat Biegon PhD, Department of Neurology, Stony Brook University School of Medicine, Stony Brook NY 11794-2565, tel: 631 632 6228 (office) 631 599 9956 (cell) fax: 631 632 6294, anat.biegon@stonybrook.eduanatbiegon@gmail.com.

other cancer and non-cancer indications in both men and women (De Ronde et al., 2011; Fedele et al., 2008; Li et al., 2008).

Several aromatase inhibitors, including vorozole ((S)-6-[(4-chlorophenyl)(1H-1,2,4-triazol-1-yl)methyl]-1-methyl-1H-benzotriazole), Ki=0.7 nM (Vanden Bossche et al., 1990) letrozole and cetrozole have been labeled with carbon-11 using [^{11}C]-methyl iodide and evaluated as radiotracers for in vivo visualization of aromatase in rodents and primates (Lidstrom et al., 1998; Takahashi et al., 2006; Kim et al., 2009; Kil et al, 2009, Biegon et al., 2010a, Pareto et al., 2013, Takahashi et al., 2014). While letrozole failed to exhibit specific uptake in baboons in vivo (Kil et al., 2009); [^{11}C]vorozole brain scans revealed high specific binding in the rhesus and baboon amygdala, similar to results obtained with autoradiography of the rat brain (Lidstrom et al., 1998; Takahashi et al., 2006; Kim et al., 2009). We have recently reinvestigated and modified the radiosynthesis and purification of [^{11}C]vorozole (Kim et al., 2009). The pure [^{11}C]vorozole was tested and validated in the brains of female baboons and was the first aromatase radiotracer used in human brain studies (Biegon et al., 2010, 2015), while both vorozole and cetrozole were used in studies of non-human primates (Lidstrom et al., 1998, Takahashi et al., 2006, Kim et al., 2009, Takahashi et al., 2014). To date, In vivo visualization of aromatase was employed to localize the enzyme in healthy rats, monkeys and human subjects as well as in the context of exposure to drugs and perturbations of homeostasis.

2. In vivo visualization of aromatase with positron emission tomography (PET)

Positron emission tomography (PET) utilizes the high energy photons formed during the annihilation of positrons to detect the changes in the amount and localization of injected radiopharmaceuticals in the living body (recently reviewed in Zanzonico, 2012). Radiolabeled molecules with known affinity and selectivity for specific tissue constituents (e.g. receptors, transporters and enzymes) are used to assess the anatomical distribution and temporal changes in target availability by measuring the amount of radioactivity in different tissues over time relative to the amount injected; or, using mathematical modeling/relative to the amount present in plasma over the same time period, corrected for metabolites. The first method, used in most clinical applications, yields standardized uptake values (SUV); where SUV (t) =measured radioactivity in tissue (Bq/ml) / injected activity (Bq)/ body weight. SUV is a dimensionless number; assuming a mass density of 1Kg/L (see recent review by Kinahan et al., 2010).

The 2nd method, in conjunction with various theoretical models, can be used to derive a number of kinetic parameters; the most commonly used being the total volume of distribution, VT (Innis et al., 2007). VT represents the distribution volume of total radiopharmaceutical uptake in tissue relative to total concentration in plasma, and is a dimensionless entity under the same assumption (1mL=1gr in tissue and blood). Both SUV and VT increases are proportional to the concentration of target available for binding the tracer; and decrease when the target is occupied by physiological or pharmacological agents which occupy the target.

2.1. PET studies in rats

In vivo visualization of aromatase in rats was performed using microPET and [^{11}C]-vorozole (Ozawa et al., 2011; Kim et al., 2009). High accumulation of [^{11}C]vorozole was detected in the stomach and the adrenal glands. In addition, ovarian uptake was observed in females, though the phase of the estrus cycle was not reported, and detectable radioactivity was also observed in male testes (Figure 1). Displacement studies and autoradiography demonstrated that aromatase was expressed in the stomach but that the accumulation of [^{11}C]vorozole in the adrenal glands might represent nonspecific binding. Interestingly, the accumulation of [^{11}C]vorozole in the stomach was significantly increased in fatigued rats (Ozawa et al 2011). The high uptake in the ovaries is to be expected since the ovaries are the main site of peripheral estrogen production. Ovarian aromatase expression, [^{11}C]vorozole binding and enzymatic activity are also strongly dependent on the stage of the estrus cycle in rats (Kirilovas et al., 2003; Stocco et al. 2008), though in vivo measurement of these changes awaits future studies comparing female rodents scanned with microPET at different stages of the cycle.

MicroPET studies of brain distribution in rats demonstrated the highest binding bilaterally in the amygdala (ratio to cerebellum, 1.7 at 40 min, n=5), with lower but significant binding in the bed nucleus of the stria terminalis. This was confirmed by ex vivo autoradiography. Pretreatment with both vorozole and letrozole blocked [^{11}C]vorozole binding in these regions, indicating specificity for brain aromatase (Figure 2). This distribution is also an excellent match to the pattern discerned by in vitro autoradiography with the same tracer (Takahashi et al., 2006).

2.2. PET studies in non-human primates

The first in vivo PET study of aromatase in monkeys (Lidstrom et al., 1998) examined the kinetics and biodistribution of [^{11}C]vorozole in two rhesus monkeys. Whole-body images revealed the highest accumulation of radioactivity in the liver, which accounted for 20% of administered radioactivity after 10 min and remained high for the duration of the scan (60 min). Early uptake, which decreased with time, was observed in the brain, lung, and kidney. Pretreatment with a pharmacological dose of vorozole resulted in a slight increase in liver uptake and a decrease in the other organs. Besides the liver, the uptake of the tracer throughout the body was relatively low and homogeneous. In view of this distribution pattern and small effects of administration of a pharmacological dose of unlabeled vorozole, the authors concluded that in vivo assessment of aromatase concentrations with [^{11}C]vorozole in peripheral tissues will be difficult.

These findings were generally replicated and extended in a subsequent study of female baboons, in which whole body distribution was examined with [^{11}C]vorozole at baseline and after pretreatment with vorozole, letrozole, or ketoconazole, a cytochrome p450 3A4 inhibitor; with lungs, heart, liver and kidneys in the field of view. Since the tracer has a chiral center and only one optical isomer is active; The R and S enantiomers were also compared. Uptake of C-11 peaked rapidly (<0.5 min) and cleared to near baseline by 6 minutes in most peripheral organs except liver, where radioactivity was very high, with slow uptake and clearance. Pretreatment with vorozole but not letrozole decreased liver binding in

a dose dependent manner. Ketoconazole, a CYP 3A4 inhibitor (Venkatakrishnan et al., 2000), also had a marked effect on liver pharmacokinetics of [^{11}C]vorozole binding although it did not completely block uptake (Kim et al., 2011).

The observation that treatment with vorozole but not letrozole reduces the monkey liver binding of [^{11}C]vorozole indicates the presence of a non-aromatase binding site which is responsible at least in part for the high liver uptake. Ketoconazole-induced changes in [^{11}C]vorozole pharmacokinetics in the liver suggest that CYP 3A4 binding, in addition to aromatase, merits consideration as a target for this tracer in the liver (Kim et al 2011). The other peripheral organ with high levels of uptake in female baboons, which was blocked by vorozole pretreatment, was the ovary (Figure 3).

A brain PET study in female rhesus macaques demonstrated the highest levels of [^{11}C]vorozole in the amygdala, where the uptake was also blocked by excess amounts of unlabeled vorozole (Takahashi et al., 2006). Measureable uptake was observed throughout the brain, though a high signal in the preoptic area was observed in only 2 out of 4 monkeys. Using the cerebellum as a reference region, the authors showed that amygdala uptake was significantly higher than uptake in temporal and occipital cortex.

A subsequent study In female baboons (Kim et al., 2009) also demonstrated the highest uptake of [^{11}C]vorozole in the amygdala (Figure 3), followed by the preoptic area and hypothalamus, basal ganglia, cortical areas and cerebellum. [^{11}C]Vorozole showed a rapid uptake by the brain followed by a relatively constant accumulation, suggesting the possibility of using the tissue to plasma ratio as an estimate of the total volume of distribution in addition to the use of kinetic modeling (Kim et al., 2009, Pareto et al., 2013). Indeed, comparison of 1 and 2 compartment models, Logan Graphical analysis (Logan et al., 2003, 2011), ratio of tissue to cerebellum and ratio of tissue to plasma all yielded a similar rank order of estimates of aromatase availability (Pareto et al., 2013). Pretreatment (“blocking”) studies with both vorozole and letrozole showed a general decrease in brain accumulation and distribution volume. The results of this study also suggested that the physiologic changes in gonadal hormone levels accompanying the menstrual cycle may have a significant effect on brain aromatase availability (Pareto et al., 2013), with lower levels associated with the high-estrogen (estrus) phase of the cycle (Figure 5). These findings suggest that in baboon, high levels of circulating estrogen may reduce brain aromatase gene expression indirectly, by affecting the levels of other physiologic mediators such as gonadotropins and cytokins, known to regulate aromatase expression (Bulun et al., 2005). Most recently, primate brain aromatase distribution was examined with the new tracer [^{11}C]cetrozole. Again, high specific binding of [^{11}C]cetrozole was observed in the amygdala and hypothalamus. In addition, the authors noted binding in the nucleus accumbens of rhesus monkeys which was not appreciated in their previous studies with [^{11}C]vorozole in this species (Takahashi et al 2014). The time–activity curves for plasma and metabolites were fitted to a 3 exponential model and a Hill function, respectively. The data with arterial blood sampling were analyzed with a Logan plot (Logan et al 2003, 2011), and the total distribution volume (V_T) in each brain region was calculated. The data without arterial blood sampling were analyzed with a Logan reference tissue model based on average k2’, using the cerebellum as a reference. Both methods of analysis resulted in a similar rank

order of regional aromatase, which was similar to the one detected by [^{11}C]vorozole in rhesus and baboon but with a higher signal to noise ratio (Takahashi et al 2014).

2.2.1. In vivo effects of hormone and drug exposure on brain aromatase in monkeys—Nicotine and other tobacco alkaloids are known to inhibit aromatase activity in vitro (Barbieri Et. al., 1986; Kadohama et al., 1993). The effect of nicotine on brain aromatase availability was examined with [^{11}C]vorozole in six female baboons before and after exposure to IV nicotine at .015 and .03 mg/kg; doses shown to produce plasma levels in the range encountered in cigarette smokers (Biegon et al., 2010). Nicotine administration produced significant, dose-dependent reductions in [^{11}C]vorozole binding. The amygdala and preoptic area showed the largest reductions (Figure 6). Thus, nicotine interacts in vivo with primate brain aromatase in regions involved in mood, aggression, and sexual behavior (Biegon et al., 2010), suggesting aromatase inhibition may contribute to the known physiological and behavioral effects of cigarette smoking (Biegon et al., 2012).

The effect of anabolic steroids was examined in male rhesus monkeys treated with nandrolone decanoate for 3 weeks, with brain aromatase examined with PET and [^{11}C]vorozole. (Takahashi et al 2011). After treatment with nandrolone, a significant increase in [^{11}C]vorozole binding was observed in the hypothalamus but not other areas including the amygdala, which is also aromatase enriched. These findings in monkeys are consistent with those obtained earlier in rats using autoradiography (Takahashi et al. 2007, 2008). These findings also suggest that aromatase in the hypothalamus may play a role in the emotional instability of anabolic-androgenic steroids abusers (Pope et al., 2000).

2.3. PET studies in healthy men and women

The most comprehensive study of aromatase distribution in healthy humans performed to date, using PET and [^{11}C]vorozole (Biegon et al., 2015), examined 13 men and 20 women (age range 23 to 67). PET data were acquired over a 90 minute period. Each subject had 4 scans, 2/day separated by 2-6 weeks, including brain and torso or pelvis scans. Young women were scanned at 2 discrete phases of the menstrual cycle (midcycle and late luteal). Men and postmenopausal women were also scanned following pretreatment with a clinical dose of the aromatase inhibitor letrozole (“blocking” studies) to validate specificity of the binding to the target. Time activity curves were obtained and standard uptake values (SUV) calculated for major organs including brain, heart, lungs, liver, kidneys, spleen, muscle, bone and male and female reproductive organs (penis, testes, uterus, ovaries). Organ and whole body radiation exposures were calculated using Olinda software (Stabin et al, 2005). Liver uptake was higher than all other organs, but was not blocked by pretreatment with letrozole. The largest SUVs in the human body were recorded from liver, followed by the brain in men and ovary in women (Biegon et al., 2015, Figure 7). Thus, mean brain SUVs in men (2.6±0.12 in thalamus) were higher than other organs in the male body (ranging from 0.48±0.05 in lungs to 1.5±0.13 in kidneys). In women, mean ovarian SUVs (3.08±0.7) were comparable to brain SUVs and higher than other organs in the female body. Furthermore, ovarian SUVs in young women around the time of ovulation (midcycle) were significantly higher than those measured in the late luteal phase, though the increases were unilateral, apparent in only one ovary/cycle. In shared organs, there was a small but significant

difference in aromatase SUVs, with values in men higher than in women (Biegon et al., 2015).

For this reason, kinetic analysis and modeling were only performed on brain scans. Kinetic analysis and modeling of regional brain uptake (Biegon et al., 2010, Logan et al., 2014) revealed a highly specific and heterogeneous pattern which appears to be unique to humans. The highest levels were seen in the thalamus, though thalamic distribution was not uniform either. Within the thalamus, the highest levels were found in the dorsomedial and pulvinar nuclei with lower density in lateral and ventral thalamic nuclei (Figures 7,8). Very high levels were also found in the paraventricular hypothalamic nucleus.

Moderately high levels of aromatase were noted in amygdala and preoptic area/anterior hypothalamus and in the medulla (inferior olive). Basal ganglia levels were relatively low, with visibly higher levels in the ventral striatum/nucleus accumbens (Biegon et al, 2010a, 2015). All cortical regions bound the tracer, with hippocampus indistinguishable from the temporal cortex. The distribution volume values derived from a 2 compartment model, graphical analysis or region/plasma ratios (Gunn et. Al., 2001, Logan et al., 2003, 2011,2014) in both men and women (regardless of menstrual cycle) all followed the same rank order: thalamus>amygdala= preoptic area> medulla(inferior olive)> cortex = hippocampus, putamen, cerebellum and white matter (Figure 8).

The specificity of the PET signal was confirmed by “blocking” experiments, in which a pharmacological dose of the specific aromatase inhibitor letrozole (2.5mg p.o), known to inhibit aromatase activity by more than 90%, was administered prior to the administration of tracer doses (less than 1% of the pharmacological dose) of the labeled vorozole. Imaging under these conditions provides the regional distribution of non-specific tracer binding, since the specific and saturable binding sites on the enzyme are fully saturated by the large excess of unlabeled letrozole. Pretreatment with letrozole reduced tracer uptake in all of the brain regions examined, resulting in a homogenous distribution across regions (Figure 8). The size of the reduction was region dependent, ranging from ~70% blocking in thalamus and preoptic area to ~10% in cerebellum (Biegon et al 2010, 2015). This indicates that the heterogeneous distribution of tracer binding in the brain is indeed indicative of region-dependent differences in the distribution of aromatase. Furthermore, the fact that non – specific binding was lower than total binding throughout the brain indicates that aromatase expression is quite ubiquitous, and most, if not all, human brain regions express aromatase.

2.3.1 Effects of endogenous hormone levels, age and cigarette smoking on human aromatase—There was no correlation between estrogen, testosterone or the estrogen/testosterone ratio and SUV in the various organs in men and postmenopausal women, although individual plasma testosterone and estrogen levels were within the established norms for adult men and women, with testosterone levels of 250-570 ng/mL in men and <20- 32 ng/mL in women and estrogen levels of <50-114 pg/mL in men and 84-250 pg/mL in premenopausal women. In premenopausal women, ovarian SUVs near the time of ovulation (midcycle, 5.0±1) were significantly higher ($p<0.05$, one way ANOVA followed by Fisher's PLSD) than those measured in the late luteal (1.5±0.2) or early follicular (1.3±0.05) phase as determined from self-report and confirmed by hormone levels.

The increased ovarian uptake at midcycle was unilateral (Figure 7B); similar to the increase observed in estrus baboons (Figure 4). Analysis of brain uptake revealed significantly lower levels in subjects over age 50 and active cigarette smokers. However, these factors did not influence the rank order of tracer distribution in the brain (Biegon et al., 2015), and the effects were considerably smaller than those seen with clinical doses of letrozole (blocking study). Interestingly, the decrease in aromatase availability with age was not linear in some brain regions, and was decidedly curvilinear in cortical white matter (Figure 9), where values reached a minimum in middle age and then increased again in the older subjects.

This study, the first to compare brain, torso and pelvis in a relatively large group of the same subjects, also resulted in the rather surprising observation that the brain of men has the highest estrogen synthesizing capacity in the male body; and the only peripheral organ with similar capacity is the female ovary during ovulation. However, unlike ovarian uptake, regional brain uptake of [^{11}C]vorozole did not vary across the menstrual cycle in premenopausal women. These results echo rodent studies showing that brain aromatase is not significantly regulated by the estrous cycle in rodents (Roselli et al., 1984)), although we did observe significant menstrual cycle dependent changes in modeled kinetic parameters in female baboon brain (Pareto et al., 2013; Figure 5). Other factors, including age, sex and cigarette smoking had significant effects on human brain uptake of [^{11}C]vorozole. Thus, small but consistent sex differences were detected in the brain, with higher values in all men relative to all women (Biegon et al., 2015). These findings resonate with similar observations obtained in rats using [^{11} C]vorozole and in vitro autoradiography (Takahashi et al., 2006).

3. Relationship between in vivo and in vitro studies of aromatase distribution in animals and humans

The results of in vivo studies of aromatase distribution under baseline conditions as well as following hormonal and pharmacological manipulations are generally consistent with in vitro studies. For example, higher aromatase levels in male relative to female brains observed in vivo are consistent with the findings of Takahashi et al., (2007, 2008) who demonstrated that androgenic-anabolic steroids increased aromatase concentration in the bed nucleus of stria terminalis and preoptic area in rat brain, as evaluated using autoradiography with [^{11}C]vorozole. A follow-up study examined whether the increase in aromatase binding is mediated via androgen receptors and whether this increase occurs in neurons or glial cells (Takahashi et al 2008). Treatment with the androgen receptor antagonist Flutamide decreased [^{11}C]vorozole binding in the bed nucleus of the stria terminalis, preoptic area, and medial amygdala, which was increased by the agonist nandrolone. Immunohistochemical examination demonstrated that androgen-mediated upregulation of aromatase expression occurred in neurons. These findings are also compatible with earlier studies showing androgen regulation of aromatase mRNA in rat brain (Abdelgadir et al., 1994).

A comparison of findings from different species yields some similarities but also significant differences in aromatase distribution. Relatively high aromatase levels in the ovary, especially around the time of ovulation, were observed in rats, monkeys and women. Prominent liver uptake was also seen across species. However, the high uptake in rat

stomach reported by Ozawa et al. (2011) was not seen in baboons or humans. Tracer uptake in the majority of most other peripheral organs, including bone, kidney, muscle, heart and lung, was uniformly low across species.

Comparison of brain distribution across species reveals a similar rank order of tracer uptake in rats, rhesus monkeys and baboons, with highest levels in amygdala. However, the distribution pattern in the human brain is starkly different, with the highest levels of aromatase detected in thalamic nuclei (mediodorsal and pulvinar); and moderate levels in the amygdala, preoptic area and medulla (Biegon et al., 2010, 2012, 2015). Low levels of aromatase are found in all other cortical and subcortical regions of all species examined (Takahashi et al., 2006, 2014, Kim et al., 2009, Biegon et al., 2010).

The most likely explanation for the species differences in aromatase distribution and the unique brain distribution in humans is the unique location, size and highly elaborate organization of the human aromatase gene (e.g. Bulun et al., 2003). The human Cyp19 is a large gene located on chromosome 15 which has 10 different tissue-specific promoters under the control of distinct physiological mediators, while the mouse gene is located on chromosome 9, is much smaller and contains a smaller number of tissue specific promoters (Kamat et al., 2002, Golovine et al., 2003, Honda et al., 2004). Since other promoters besides the brain specific exon 1.f (Sasano et al 1998) are expressed in the human brain, this heterogeneity may also provide the basis for brain region specific regulation of aromatase.

Comparing in vivo and postmortem results in humans is more difficult since the methodologies used do not include autoradiography or direct binding of inhibitors, and therefore are not as comparable to PET results. Furthermore, postmortem studies in humans generally included a relatively small number of regions and subjects. With these caveats in mind, the post mortem and in vivo findings are generally compatible. Thus, aromatase gene expression was examined in postmortem samples from eight brain regions (Sasano et al., 1998). The amount of aromatase mRNA determined by RT-PCR assay in 6 cases (4 men, 2 women) was highest in pons, thalamus, hypothalamus and hippocampus. Analysis of multiple exons 1 revealed that exons I.f, considered specific for brain, as well as the fibroblast type and gonadal type (Bulun et al., 2003), were expressed in the brain. Both the gonadal and brain types tended to be utilized in hypothalamus, thalamus and amygdala. The amount of overall mRNA expression was also higher in hypothalamus, thalamus and amygdala than in other regions of the brain. There were no differences of utilization of exons 1 and mRNA expression of aromatase between female and male brain. The authors conclude that their results demonstrate that aromatase is expressed widely in human brain tissues in both men and women. The presence of aromatase transcripts in human temporal cortex, frontal cortex and hippocampus was also confirmed by Stoffel-Wagner et. al. (1999). Aromatase immunoreactivity was found in hypothalamus, amygdala, preoptic area and (cholinergic) ventral forebrain nuclei by Ishunina et al. (2005). More recent studies confirmed aromatase immunoreactivity in temporal cortex, hippocampus and prefrontal cortex (Yague et al., 2006, Yague et al., 2010). Immunohistochemistry was also used to examine the cellular and subcellular distribution of aromatase in the human brain, establishing the presence of aromatase immunoreactivity in neurons as well as in glia. Thus, cortical and hippocampal aromatase was detected in pyramidal cells, granule cells and

interneurons; in perikarya, dendrites, axons and axon terminals (Naftolin et al., 1996, Yague et al., 2006, Yague et al., 2010). The presence of glial aromatase was confirmed in prefrontal cortex, temporal cortex and hippocampus, where it was associated with astrocytes (Yaggue et al., 2006, Yague et al., 2010).

Aromatase enzymatic activity was first described in the fetal human limbic system by Naftolin et al., (1971), followed by reports on activity in the adult brain and temporal cortex (Naftolin et al., 1996; Steckelbroeck et al., 1999). These findings are in broad agreement with the in vivo observations on the gross anatomical level, showing aromatase is present throughout the brain.

Previous studies on postmortem brain samples (e.g. Sasano et al., 1998. Steckelbroeck et al., 1999, Stoffel-Wagner et al., 1999) did not note sex differences or age effects on brain aromatase activity and gene expression in men and women, while the results of the in vivo studies described above do suggest a small but consistent sex difference and age effects, with higher levels in men (compatible with findings in rats) and an age–dependent decrease in most brain regions. The discrepancy most likely reflects issues of statistical power since previous human studies, including published pilot data from the same series (Biegon et al., 2010) examined a much smaller number of subjects (32 vs. less than 10).

4. Current limitations and future directions

There are several limitations associated with PET imaging of aromatase using carbon-11 labeled aromatase inhibitors. Due to the very short half-life of carbon 11 (20 minutes), PET studies with currently available, validated tracers can only be performed in medical or research centers in possession of a cyclotron, which represent only a small percentage of hospitals, most of which do possess PET scanners. This problem can only be overcome by the development and validation of aromatase tracers labeled with a longer-lived isotope such as Fluorine-18 (Erlandsson et al., 2008).

A Fluorine-18 labeled aromatase tracer may also address the difficulty encountered in quantification of aromatase content in the majority of peripheral organs, which express aromatase at relatively low levels. [^{11}C]vorozole binding to aromatase in vivo is slow, such that good signal-to-noise ratios are only obtained 50-90 minutes after administration, at which point the absolute counts are quite low and low uptake tissues are hard to visualize. However, the low uptake in the majority of peripheral organs (all besides the liver) may actually be an advantage if the tracers are used to detect primary tumors overexpressing aromatase or their metastases in breast, lung, bone and most of the brain.

It is also important to remember that PET with aromatase inhibitors is useful in detecting changes in aromatase availability but not in enzyme activity. While it is true that no estrogen is produced in the absence of aromatase, changes in enzyme activity can result in increases or decreases in tissue estrogen levels with no change in aromatase expression. In fact, such changes have been shown to occur relatively quickly and appear to account for at least some behaviors related to estrogen in the brain of animals (Cornil et al., 2013, Dickens et al., 2014). To gain a complete picture of normal and abnormal changes in regional estrogen synthesis capacity, it would be advantageous to develop radiotracers which are substrates

rather than non-competitive inhibitors of the enzyme. The development of the synthetic LDOPA decarboxylase substrate 6-[18F]-fluoro-3,4-dihydroxyphenyl -L-alanine ([^{18}F]-DOPA) was an early success in this regard (Garnett et al. 1983, also see Holland et al. 2013 for a recent review).

Despite these caveats, the results of the studies reviewed here demonstrate that in vivo measurement of aromatase distribution by PET is reproducible across tracers and research centers and that aromatase distribution is regulated in a species, sex, organ- and brain-region specific manner. The PET signal produced by currently available radiolabeled aromatase inhibitors is specific and sensitive to physiological and pharmacological manipulation of the enzyme in organs and regions containing moderate to high enzyme concentrations.

The ability to measure aromatase content non-invasively throughout the human body and in distinct brain regions offers an unprecedented opportunity to determine the involvement of this enzyme in multiple physiological and pathological conditions; since aromatase, along with specific estrogen receptors, has been implicated in cellular proliferation, reproduction, sexual differentiation, sexual behavior, aggression, cognition, memory and neuroprotection in various animal species (McEwen et al., 1977, Sierra et al., 2003, Trainor et al., 2006, Garcia-Segura 2008, Saldahana et al., 2009, Roselli et al., 2009).

In humans, postmortem studies have also shown that aromatase expression in the brain and aromatase genotype are linked to Alzheimer's disease (Ishunina et al., 2005, Livonen et al., 2004, Huang et al., 2006, Hiltunen et al., 2006) and autism (Sarachana et al, 2011, 2013)

In addition, increases in aromatase expression are implicated in a wide range of peripheral human diseases, most prominently in breast cancer (Bulun et al., 2008), but also other pathologies including endometriosis (Fedele et al., 2008) brain, lung and hepatic cancer (Wozniak et al., 1998, Marguez-Garban et al., 2009, Micelli et al., 2009) and unexplained female infertility (Mitwally and Casper 2003).

Future studies with [11C]vorozole PET in these and additional disorders have the potential of identifying aromatase as a treatment target in disorders which are not currently treated with aromatase inhibitors, to improve early detection of aromatase-overexpressing tumors and help identify patients more likely to respond to AI therapy, while preventing unnecessary exposure to the adverse effects of AI (osteroporosis, hot flushes, musculoskeletal disorders, fatigue and mood disturbances among others, e.g. Mouridsen et al., 2003). Resistance to endocrine treatment is another clinical area where [11C]vorozole PET may have a significant impact. Although the mechanisms underlying resistance are not fully understood (Chumsri et al., 2014), treatment-related increases in aromatase expression (Catalano et al 2014) is a likely mechanism which can be detected with aromatase imaging. [11C]vorozole PET will also provide a tool for early determination of target engagement, pharmacokinetics and pharmacodynamics of new AI drugs in development (Hietala 1999, Waarde 2000).

Acknowledgement

Supported in part by NIH 1R21EB012707 (Biegon, Anat PI)

References

Abdelgadir SE, Resko JA, Ojeda SR, Lephart ED, McPhaul MJ, Roselli CE. Androgens regulate aromatase cytochrome P450 messenger ribonucleic acid in rat brain. Endocrinology. 1994; 135:395–401. [PubMed: 8013375]

Azcoitia I, Yague JG, Garcia-Segura LM. Estradiol synthesis within the human brain. Neuroscience. 2011; 191:139–47. [PubMed: 21320576]

Barbieri RL, Gochberg J, Ryan KJ. Nicotine, cotinine, and anabasine inhibit aromatase in human trophoblast in vitro. J Clin Invest. 1986; 77:1727–1733. [PubMed: 3711333]

Biegon A, Kim SW, Logan J, Hooker JM, Muench L, Fowler JS. Nicotine blocks brain estrogen synthase (aromatase): in vivo positron emission tomography studies in female baboons. Biol Psychiatry. 2010a; 67:774–777. [PubMed: 20188349]

Biegon A, Kim SW, Alexoff DL, Jayne M, Carter P, Hubbard B, King P, Logan J, Muench L, Pareto D, Schlyer D, Shea C, Telang F, Wang GJ, Xu Y, Fowler JS. Unique distribution of aromatase in the human brain: in vivo studies with PET and [N-methyl-11C]vorozole. Synapse. 2010b; 64:801–807. [PubMed: 20842717]

Biegon, A.; Fowler, J.; Kim, S-W.; Logan, J.; Pareto, D.; Wang, GJ. Distribution of aromatase in the human brain.. In: Balthazart, J.; Ball, JF., editors. Brain aromatase, estrogens and behavior. Oxford University Press; 2012. p. 89-99.

Biegon A, Alia-Klein N, Fowler JS. Potential contribution of aromatase inhibition to the effects of nicotine and related compounds on the brain. Front Pharmacol. 2012; 3:185. doi: 10.3389/fphar.2012.00185. eCollection 2012. [PubMed: 23133418]

Biegon A, Alexoff DL, Kim S-W, Logan J, Pareto D, Schlyer D, Wang G-J, Fowler JS. Aromatase Imaging with [N-methyl-C-11]vorozole PET in Healthy Men and Women. J. Nuc Med. 2015; 56:580–585.

Bulun SE, Simpson ER. Aromatase expression in women's cancers. Adv Exp Med Biol. 2008; 630:112–132. [PubMed: 18637488]

Bulun SE, Sebastian S, Takayama K, Suzuki T, Sasano H, Shozu M. The human CYP19 (aromatase P450) gene: update on physiologic roles and genomic organization of promoters. J Steroid Biochem Mol Biol. 2003; 86:219–224. [PubMed: 14623514]

Bulun SE, Lin Z, Imir G, Amin S, Demura M, Yilmaz B, Martin R, Utsunomiya H, Thung S, Gurates B, Tamura M, Langoi D, Deb S. Regulation of aromatase expression in estrogen-responsive breast and uterine disease: from bench to treatment. Pharmacol Rev. 2005; 57:359–83. [PubMed: 16109840]

Buzdar A, Howell A. Advances in aromatase inhibition: clinical efficacy and tolerability in the treatment of breast cancer. Clin Cancer Res. 2001; 7:2620–2635. [PubMed: 11555572]

Catalano S, Giordano C, Panza S, Chemi F, Bonofiglio D, Lanzino M, Rizza P, Romeo F, Fuqua SA, Maggiolini M, Andò S, Barone I. Tamoxifen through GPER upregulates aromatase expression: a novel mechanism sustaining tamoxifen-resistant breast cancer cell growth. Breast Cancer Res Treat. 2014; 146:273–285. [PubMed: 24928526]

Chumsri S, Schech A, Chakkabat C, Sabnis G, Brodie A. Advances in mechanisms of resistance to aromatase inhibitors. Expert Rev Anticancer Ther. 2014; 14:381–93. [PubMed: 24559291]

Cohen MH, Johnson JR, Li N, Chen G, Pazdur R. Approval summary: Letrozole in the treatment of postmenopausal women with advanced breast cancer. Clin Cancer Res. 2002; 8:665–669. [PubMed: 11895893]

Cornil CA, Seredynski AL, de Bournonville C, Dickens MJ, Charlier TD, Ball GF, Balthazart J. Rapid control of reproductive behaviour by locally synthesisedoestrogens: focus on aromatase. J Neuroendocrinol. 2013; 25:1070–8. [PubMed: 23763492]

De Ronde W, d De Jong FH. Aromatase inhibitors in men: effects and therapeutic options. Reprod Biol Endocrinol. 2011; 9:93–99. [PubMed: 21693046]

Dickens MJ, de Bournonville C, Balthazart J, Cornil CA. Relationships between rapid changes in local aromatase activity and estradiol concentrations in maleand female quail brain. Horm Behav. 2014; 65:154–64. [PubMed: 24368290]

Erlandsson M, Karimi F, Takahashi K, Langstrom B. 18F-labeled vorozole analogues as PET tracer for aromatase. JLCR. 2008; 51:207–212.

Fedele L, Somigliana E, Frontino G, Benaglia L, Vigano P. New drugs in development for the treatment of endometriosis. Expert Opin Investig Drugs. 2008; 17:1187–202.

Garcia-Segura LM. Aromatase in the brain: not just for reproduction anymore. J Neuroendocrinol. 2008; 20:705–712. [PubMed: 18601693]

Garnett S, Firnau G, Nahmias C, Chirakal R. Striatal dopamine metabolism in living monkeys examined by positron emission tomography. Brain Res. 1983; 280:169–171. [PubMed: 6418330]

Golovine K, Schwerin M, Vanselow J. Three different promoters control expression of the aromatase cytochrome p450 gene (cyp19) in mouse gonads and brain. Biol Reprod. 2003; 68:978–984. [PubMed: 12604651]

Gunn RN, Gunn SR, Cunningham VJ. Positron emission tomography compartmental models. J Cereb Blood Flow Metab. 2001; 21:635–652. [PubMed: 11488533]

Hietala J. Ligand-receptor interactions as studied by PET: implications for drug development. Ann Med. 1999; 31:438–43. [PubMed: 10680859]

Hiltunen M, Iivonen S, Soininen H. Aromatase enzyme and Alzheimer's disease. Minerva Endocrinol. 2006; 31:61–73. [PubMed: 16498364]

Holland JP, Cumming P, Vasdev N. PET radiopharmaceuticals for probing enzymes in the brain. Am J Nucl Med Mol Imaging. 2013; 3:194–216. [PubMed: 23638333]

Honda S, Harada N, Takagi Y. Novel exon 1 of the aromatase gene specific for aromatase transcripts in human brain. Biochem Biophys Res Commun. 1994; 198:1153–1160. [PubMed: 8117272]

Howell A, Cuzick J, Baum M, et al. Results of the ATAC (Arimidex, Tamoxifen, Alone or in Combination) trial after completion of 5 years' adjuvant treatment for breast cancer. Lancet. 2005; 365:60–62. [PubMed: 15639680]

Huang R, Poduslo SE. CYP19 haplotypes increase risk for Alzheimer's disease. J Med Genet. 2006; 43:e42. [PubMed: 16882736]

Innis RB, Cunningham VJ, Delforge J. Consensus nomenclature for in vivo imaging of reversibly binding radioligands. J Cereb Blood Flow Metab. 2007; 27:1533–9. [PubMed: 17519979]

Ishunina TA, Van Beurden D, Van Der Meulen G, Unmehopa UA, Hol EM, Huitinga I, Swaab DF. Diminished aromatase immunoreactivity in the hypothalamus, but not in the basal forebrain nuclei in Alzheimer's disease. Neurobiol Aging. 2005; 26:173–194. [PubMed: 15582747]

Iivonen S, Corder E, Lehtovirta M, Helisalmi S, Mannermaa A, Vepsalainen S, Hanninen T, Soininen H, Hiltunen M. Polymorphisms in the CYP19 gene confer increased risk for Alzheimer disease. Neurology. 2004; 62:1170–1176. [PubMed: 15079018]

Kadohama N, Shintani K, Osawa Y. Tobacco alkaloid derivatives as inhibitors of breast cancer aromatase. Cancer Lett. 1993; 75:175–182. [PubMed: 8313352]

Kamat A, Hinshelwood MM, Murry BA, Mendelson CR. Mechanisms in tissue-specific regulation of estrogen biosynthesis in humans. Trends Endocrinol Metab. 2002; 13:122–128. [PubMed: 11893526]

Kil KE, Biegon A, Ding YS, Fischer A, Ferrieri RA, Kim SW, Pareto D, Schueller MJ, Fowler JS. Synthesis and PET studies of [(11)C-cyano]letrozole (Femara), an aromatase inhibitor drug. Nucl Med Biol. 2009; 36:215–223. [PubMed: 19217534]

Kim SW, Biegon A, Katsamanis ZE, Ehrlich CW, Hooker JM, Shea C, Muench L, Xu Y, King P, Carter P, Alexoff DL, Fowler JS. Reinvestigation of the synthesis and evaluation of [N-methyl-(11)C]vorozole, a radiotracer targeting cytochrome P450 aromatase. Nucl Med Biol. 2009; 36:323–334. [PubMed: 19324278]

Kim, S-W.; Alexoff, D.; Dhawan, J.; Biegon, A.; Hooker, JM.; Dewey, SL.; Fowler, JS. Evaluation of aromatase (estrogen synthase) in rodent brain using C-11 vorozole and microPET. Society for Neuroscience; Chicago: 2009. Program No. 771.14 Abstract Viewer/Itinerary PlannerOnline

Kinahan PE, Fletcher JW. Positron emission tomography-computed tomography standardized uptake values in clinical practice and assessing response to therapy. Semin Ultrasound CT MR. 2010; 31:496–505. [PubMed: 21147377]

Kirilovas D, Naessen T, Bergström M, Bergström-Petterman E, Carlström K, Långström B. Characterization of [^{11}C]vorozole binding in ovarian tissue in rats throughout estrous cycle in

association with conversion of androgens to estrogens in vivo and in vitro. Steroids. 2003; 68:1139–46. [PubMed: 14643875]

Kim S-W, Anat Biegon A, Hooker J, VanAlstine M, Logan J, Volkow N, Fowler J. Saturable, non-aromatase binding of [^{11}C]vorozole in baboon liver. J Nucl Med. 2011; 52(Supplement 1):416.

Li YF, Hu W, Fu SQ, Li JD, Liu JH, Kavanagh JJ. Aromatase inhibitors in ovarian cancer: Is there a role? Int J Gynecol Cacer. 2008; 18:600–614.

Lidstrom P, Bonasera TA, Kirilovas D, Lindblom B, Lu L, Bergstrom E, Bergstrom M, Westlin JE, Langstrom B. Synthesis, in vivo rhesus monkey biodistribution and in vitro evaluation of a 11C-labelled potent aromatase inhibitor: [N-methyl-11C]vorozole. Nucl Med Biol. 1998; 25:497–501. [PubMed: 9720668]

Logan J. A review of graphical methods for tracer studies and strategies to reduce bias. Nucl Med Biol. 2003; 30:833–844. [PubMed: 14698787]

Logan J, Alexoff D, Fowler JS. The use of alternative forms of graphical analysis to balance bias and precision in PET images. J Cereb Blood Flow Metab. 2011; 31:535–546. [PubMed: 20808318]

Logan J, Pareto D, Fowler J, Biegon A. Kinetic analysis of ^{11}C-vorozole Binding in the Human Brain with PET. Mol Imaging. 2014; 13::1–12. [PubMed: 24824855]

Márquez-Garbán DC, Hsiao-Wang, Chen HW, Lee, Goodglick L, Michael C, Fishbein MC, Pietras RJ. Targeting aromatase and estrogen signaling in human non-small cell lung cancer. Ann N Y Acad Sci. 2009; 1155:194–205. [PubMed: 19250205]

McEwen BS, Lieberburg I, Chaptal C, Krey LC. Aromatization: important for sexual differentiation of the neonatal rat brain. Horm Behav. 1977; 9:249–263. [PubMed: 611076]

Miceli V, Cervello M, Azzolina A, Montalto G, Calabrò M, Carruba G. Aromatase and amphiregulin are correspondingly expressed in human liver cancer cells. Ann N Y Acad Sci. 2009; 1155:252–256. [PubMed: 19250212]

Mitwally MF, Casper RF. Aromatase inhibition reduces gonadotrophin dose required for controlled ovarian stimulation in women with unexplained infertility. Hum Reprod. 2003; 18:1588–1597. [PubMed: 12871867]

Mouridsen HT. Incidence and management of side effects associated with aromatase inhibitors in the adjuvant treatment of breast cancer in postmenopausal women. Curr Med Res Opin. 2006; 22:1609–1621. [PubMed: 16870085]

Ozawa M, Takahashi K, Akazawa KH, Takashima T, Nagata H, Doi H, Hosoya T, Wada Y, Cui Y, Kataoka Y, Watanabe Y. PET of aromatase in gastric parietal cells using 11C-vorozole. J Nucl Med. 2011; 52:1964–1969. [PubMed: 22072705]

Naftolin F, Horvath TL, Jakab RL, Leranth C, Harada N, Balthazart J. Aromatase immunoreactivity in axon terminals of the vertebrate brain. An immunocytochemical study on quail, rat, monkey and human tissues. Neuroendocrinology. 1996; 63:149–155. [PubMed: 9053779]

Naftolin F, Ryan KJ, Petro Z. Aromatization of androstenedione by limbic system tissue from human foetuses. J Endocrinol. 1971; 51:795–796. [PubMed: 5138326]

Pareto D, Biegon A, Alexoff D, Carter P, Shea C, Muensch L, Fowler J, Kim S-W, Logan J. In vivo imaging of brain aromatase in female baboons: ^{11}C-vorozole kinetics and effect of menstrual cycle. Molecular Imaging. 2013; 12:518–524.

Pope HG Jr, Kouri EM, Hudson JI. Effects of supraphysiologic doses of testosterone on mood and aggression in normal men: a randomized controlled trial. Arch Gen Psychiatry. 2000; 57:133–40. [PubMed: 10665615]

Roselli CE, Ellinwood WE, Resko JA. Regulation of brain aromatase activity in rats. Endocrinology. 1984; 114:192–200. [PubMed: 6537806]

Roselli CE, Liu M, Hurn PD. Brain aromatization: classic roles and new perspectives. Semin Reprod Med. 2009; 27:207–217. [PubMed: 19401952]

Rossmanith WG, Ruebberdt W. What causes hot flushes? The neuroendocrine origin of vasomotor symptoms in the menopause. Gynecol Endocrinol. 2009; 25:303–14. [PubMed: 19903037]

Sarachana T, Xu M, Wu R-C, Hu VW. Sex Hormones in Autism: Androgens and Estrogens Differentially and Reciprocally Regulate RORA, a Novel Candidate Gene for Autism. PLoS ONE. 2011; 6:e17116. [PubMed: 21359227]

Sarachana T, Hu VW. Genome-wide identification of transcriptional targets of RORA. Molecular Autism. 2013; 4:14. [PubMed: 23697635]

Sasano H, Takashashi K, Satoh F, Nagura H, Harada N. Aromatase in the human central nervous system. Clin Endocrinol (Oxf). 1998; 48:325–329. [PubMed: 9578823]

Sierra A, Azcoitia I, Garcia-Segura L. Endogenous estrogen formation is neuroprotective in model of cerebellar ataxia. Endocrine. 2003; 21:43–51. [PubMed: 12777702]

Simpson ER, Clyne C, Rubin G, et al. Aromatase-A brief overview. Annu Rev Physiol 2002. 2002; 64:93–127.

Stocco C. Aromatase expression in the ovary: hormonal and molecular regulation. Steroids. 2008; 73:473–87. [PubMed: 18321551]

Steckelbroeck S, Heidrich DD, Stoffel-Wagner B, Hans VH, Schramm J, Bidlingmaier F, Klingmuller D. Characterization of aromatase cytochrome P450 activity in the human temporal lobe. J Clin Endocrinol Metab. 1999; 84:2795–2801. [PubMed: 10443682]

Stoffel-Wagner B, Watzka M, Schramm J, Bidlingmaier F, Klingmuller D. Expression of CYP19 (aromatase) mRNA in different areas of the human brain. J Steroid Biochem Mol Biol. 1999; 70:237–241. [PubMed: 10622413]

Takahashi K, Bergstrom M, Frandberg P, Vesstrom EL, Watanabe Y, Langstrom B. Imaging of aromatase distribution in rat and rhesus monkey brains with [11C]vorozole. Nucl Med Biol. 2006; 33:599–605. [PubMed: 16843834]

Takahashi K, Hosoya T, Onoe K, Doi H, Nagata H, Hiramatsu T, Li XL, Watanabe Y, Wada Y, Takashima T, Suzuki M, Onoe H, Watanabe Y. 11C-cetrozole: an improved C-11C-methylated PET probe for aromatase imaging in the brain. J Nucl Med. 2014; 55:852–857. [PubMed: 24676756]

Takahashi K, Onoe K, Doi H, Nagata H, Yamagishi G, Hosoya T, Tamura Y, Wada Y, Yamanaka H, Yokoyama C, Mizuma H, Takashima T, Bergström M, Onoe H, Långström B, Watanabe Y. Increase in hypothalamic aromatase in macaque monkeys treated with anabolic-androgenic steroids: PET study with [11C]vorozole. Neuroreport. 2011; 22:326–330. [PubMed: 21460751]

Takahashi K, Hallberg M, Magnusson K, Nyberg F, Watanabe Y, Långström B, Bergström M. Increase in [11C]vorozole binding to aromatase in the hypothalamus in rats treated with anabolic androgenic steroids. Neuroreport. 2007; 18:171–174. [PubMed: 17301684]

Takahashi K, Tamura Y, Watanabe Y, Långström B, Bergström M. Alteration in [11C]vorozole binding to aromatase in neuronal cells of rat brain induced by anabolic androgenic steroids and flutamide. Neuroreport. 2008; 19:431–435. [PubMed: 18287941]

Trainor BC, Kyomen HH, Marler CA. Estrogenic encounters: how interactions between aromatase and the environment modulate aggression. Front Neuroendocrinol. 2006; 27:170–179. [PubMed: 16376420]

Vanden Bossche H, Willemsens G, Roels I, et al. R76713 and enantiomers: selective nonsteroidal inhibitors of the cytochrome P450-dependent oestrogen synthesis. Biochem Pharmacol. 1990; 40:1707–1718. [PubMed: 2242008]

Venkatakrishnan K, von Moltke LL, Greenblatt DJ. Effects of the antifungal agents on oxidative drug metabolism—clinical relevance. Clin Pharmacokinet. 2000; 38:111–180. [PubMed: 10709776]

Waarde AV. Measuring receptor occupancy with PET. Curr Pharm Des. 2000; 6:1593–1610. [PubMed: 10974155]

Wozniak A, Hutchison RE, Morris CM, Hutchison JB. Neuroblastoma and Alzheimer's disease brain cells contain aromatase activity. Steroids. 1998; 63:263–267. [PubMed: 9618782]

Yague JG, Azcoitia I, Defelipe J, Garcia-Segura LM, Munoz A. Aromatase expression in the normal and epileptic human hippocampus. Brain Res. 2010; 1315:41–52. [PubMed: 19815003]

Yague JG, Munoz A, De Monasterio-Schrader P, Defelipe J, Garcia-Segura LM, Azcoitia I. Aromatase expression in the human temporal cortex. Neuroscience. 2006; 138:389–401. [PubMed: 16426763]

Zanzonico P. Principles of nuclear medicine imaging: planar, SPECT, PET, multi-modality, and autoradiography systems. Radiat Res. 2012; 177:349–364. [PubMed: 22364319]

Highlights

- Aromatase can be visualized *in vivo* using PET and [11C]vorozole
- Aromatase concentrations are slightly higher in males than in females
- Highest brain concentrations are found in rat and monkey amygdala and human thalamus
- Liver has high non specific uptake of radioactivity in all species following {11C]vorozole administration
- Aromatase PET may improve diagnosis and treatment in brain disorders and cancer

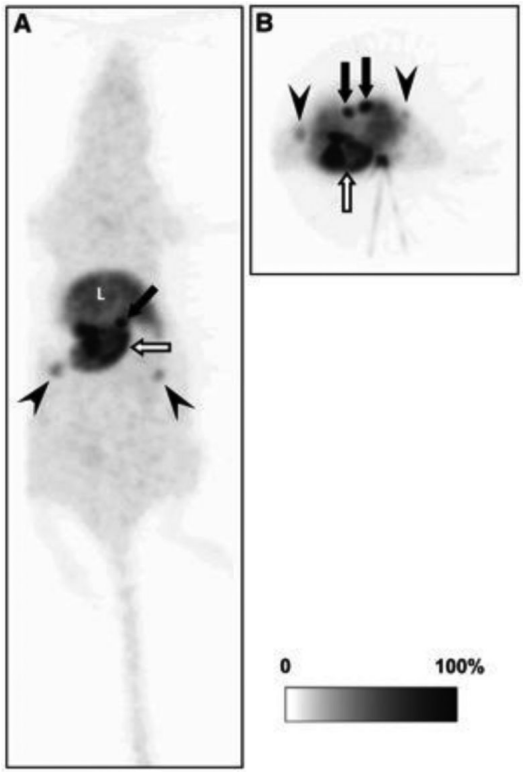

Figure 1. In vivo distribution of aromatase in the rat body

Representative whole-body maximum-intensity-projection image of 11C-vorozole in female rat: coronal (A) and transverse (B) images. 11C-vorozole was highly accumulated in stomach (open arrows), adrenal glands (closed arrows), and ovarium (arrowheads). L = liver.

This research was originally published in JNM. Ozawa M, Takahashi K, Akazawa KH, Takashima T, Nagata H, Doi H, Hosoya T, Wada Y, Cui Y, Kataoka Y, Watanabe Y. PET of aromatase in gastric parietal cells using 11C-vorozole. J Nucl Med. 2011 Dec;52(12): 1964-9. © by the Society of Nuclear Medicine and Molecular Imaging, Inc.

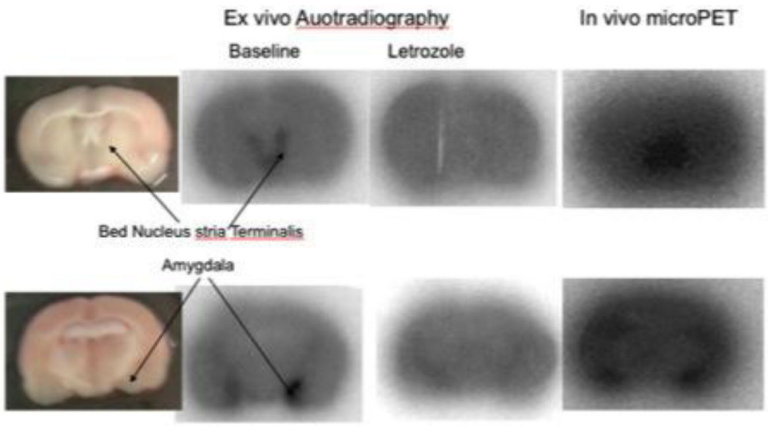

Figure 2. In vivo and ex vivo distribution of [11C]vorozole in the rat brain

Adult male rats were injected with ~0.5mCi of [^{11}C]vorozole and scanned in a microPET for 60 minutes (right column). The brains were removed, sliced in a tissue slicer and the slices photographed (leftmost column), dried and exposed to a phosphoimager screen for 40 minutes. (2nd column from left). Two animals were injected with letrozole prior to the administration of the radiotracer (blocking study, 3rd column from left).

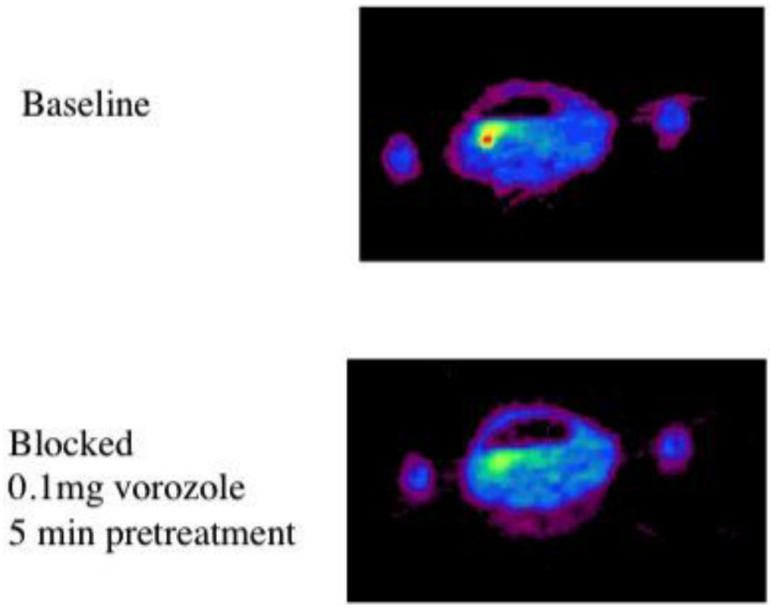

Figure 3. Specific Ovarian uptake of [11C]vorozole in the baboon ovary

Pseudocolred (rainbow spectrum) images of the pelvic region of a female baboon imaged at baseline (top) and later the same day following injection of a blocking dose of vorozole.

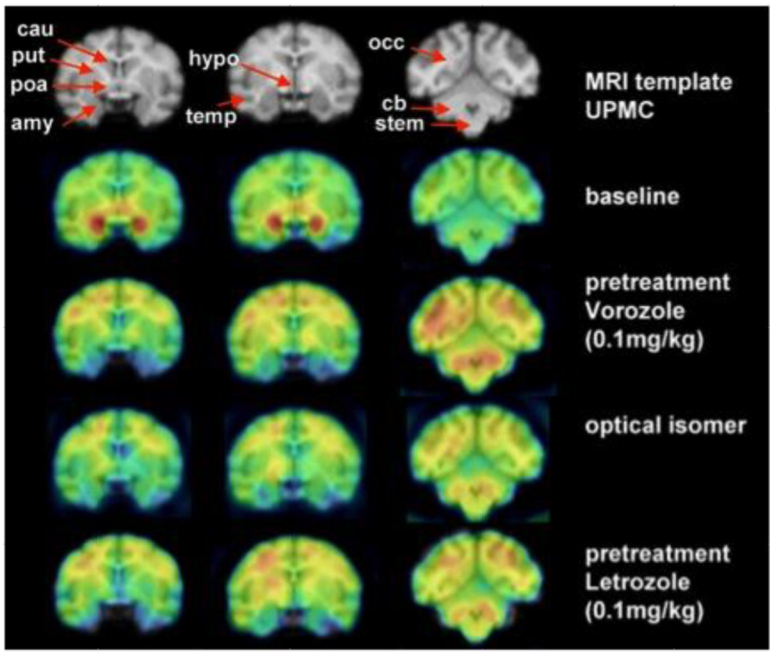

Figure 4. Regional Distribution and specificity of [11C]vorozole uptake in the female baboon brain

The upper row shows the magnetic resonance imaging (MRI) coronal sections of the template chosen. Regions of interest (ROI) are indicated with an arrow. The second row shows a baseline positron emission tomographic study (summed frames minutes 20–90) overlayed on the MRI template. The third row shows a pretreatment study with vorozole (0.1 mg/kg) followed by a study where the inactive optical isomer was labeled and injected. The last row shows the distribution when pretreatment was done with letrozole (0.1 mg/kg). amy = amygdala; cau = caudate; cb = cerebellum; cwm = cortical white matter; occ occipital cortex; poa = preoptic area; put = putamen; stem = brainstem; temp = temporal cortex. Note that pharmacological doses of vorozole and letrozole increase the levels of free tracer in plasma (probably due to competition for binding to blood cells) so the levels in brain are increased as well; but specific binding (represented as ratio of region to plasma, or ratio to cerebellum, or VT) is not increased (Pareto et al; 2013)

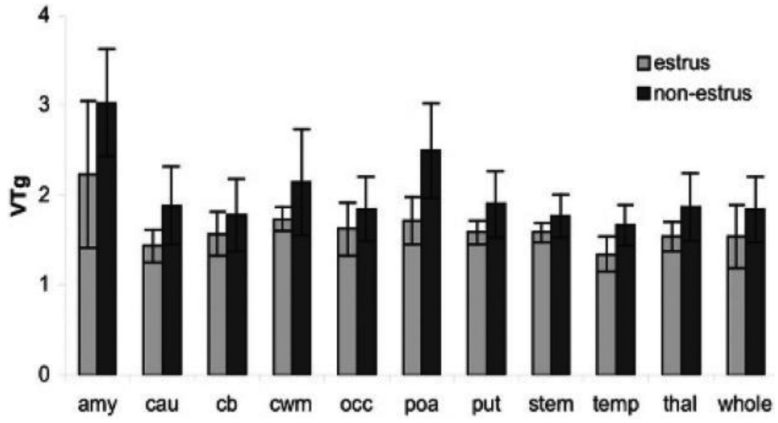

Figure 5. Effect of estrus cycle on [11C]vorozole distribution in female baboon brain

Bars represent mean values in studies performed when animals were in estrus compared to studies performed when the same animals were not in estrus. The graph depicts the regional values of the total distribution volume obtained from Logan graphical analysis (VTg). Two way analysis of variance by region and stage of cycle revealed significant effects of both ($p = .001$) on VTg, with a non-significant phase × region interaction ($p = .08$). amy = amygdala; cau = caudate; cb = cerebellum; cwm = cortical white matter; occ occipital cortex; poa = preoptic area; put = putamen; stem = brainstem; temp = temporal cortex; thal = thalamus; whole = whole brain.

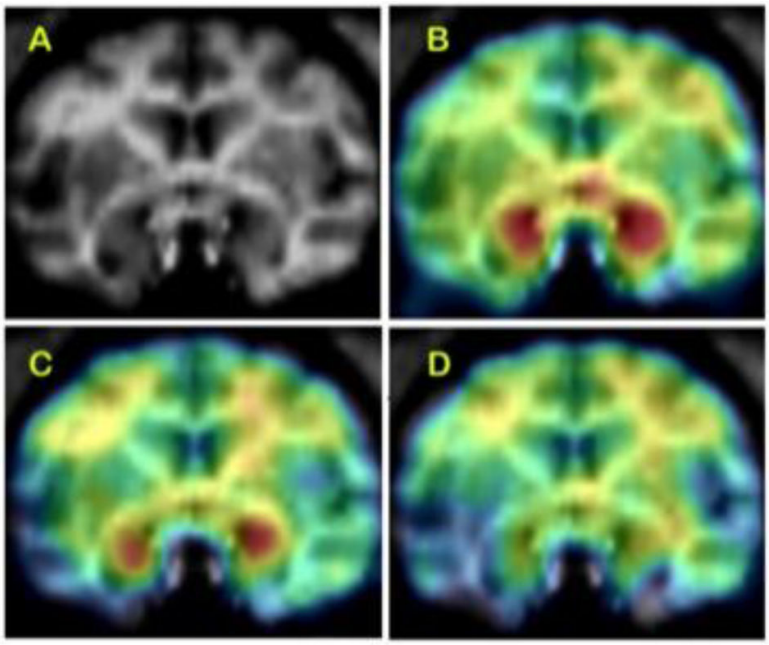

Figure 6. Effect of nicotine on brain aromatase availability in female baboon brain

Top: (A) baboon brain magnetic resonance imaging (MRI), coronal section at the level of amygdala. (B) Representative baseline positron emission tomography (PET) image coregistered with MRI. (C) The PET image of same baboon after low-dose nicotine (.015 mg/kg), coregistered with MRI. (D) The PET image after injection of high-dose (.03 mg/kg) nicotine, coregistered with MRI. The PET images show dose-corrected averaged frames acquired between 52.5 and 90 min after tracer injection, pseudocolored with the rainbow spectrum, with purple indicating the lowest density and red indicating the highest density of radioactivity.

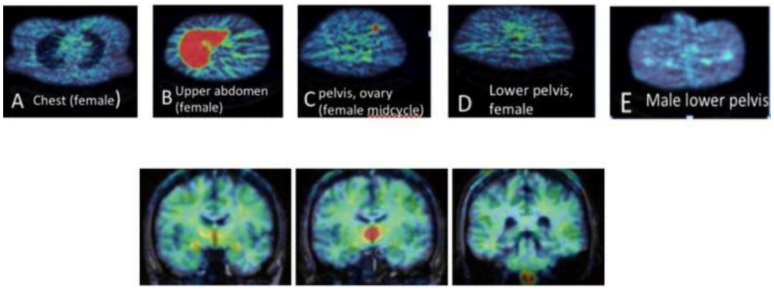

Figure 7. Distribution of aromatase in the human body and brain

Pseudocolored (rainbow spectrum) examples of 11C-vorozole uptake in body and brain. For anatomical verification, peripheral organ axial images (A-E) were overlaid on the attenuation scan obtained immediately prior to the emission scan. A. Female, level of breasts and lungs. B. Female, liver C. Female at midcycle, level of ovary. D. Female, lower pelvis. E. Male, lower pelvis. Brain coronal images (F-H) were coregistered and overlaid on a brain MRI obtained separately. F. Level of amygdala G. Level of thalamus H. Level of medulla.

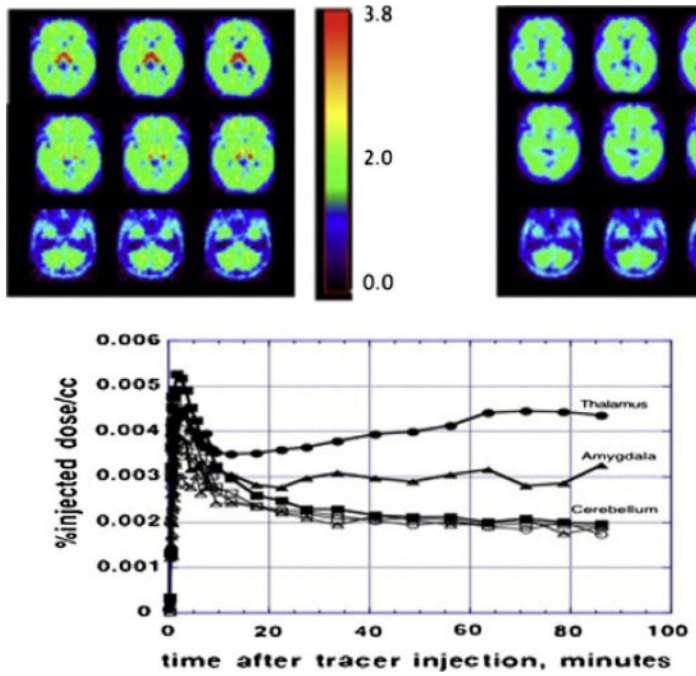

Figure 8. Specificity of [11C]vorozole uptake in the human brain

The top panels show a parametric (VT, total volume of distribution) image at baseline (left) and following ingestion of a pharmacological dose of letrozole (right). Representative time activity curves from 3 brain regions at baseline (filled symbols) and post letrozole (empty symbols) are shown in the bottom panel.

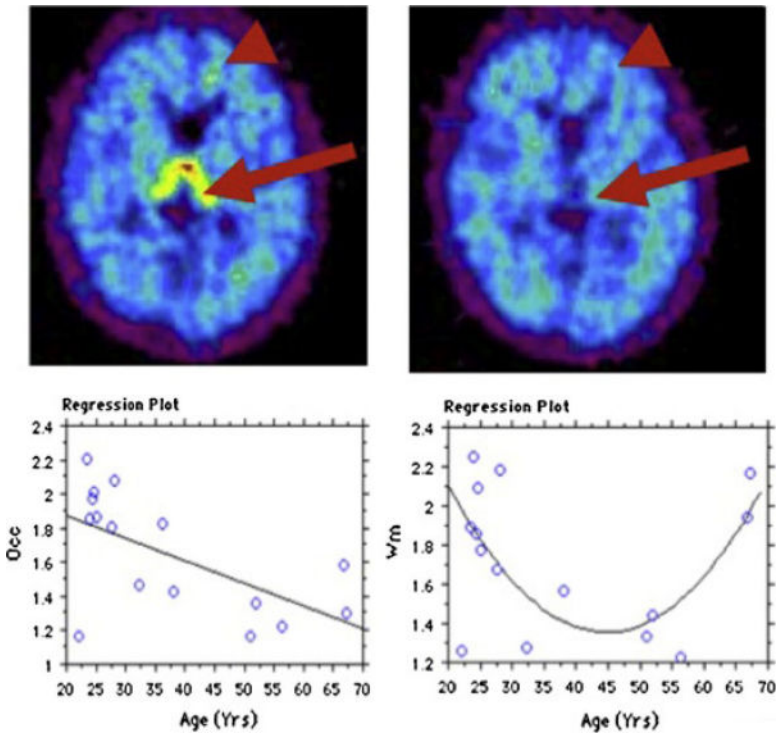

Figure 9. Effect of aging on aromatase availability in the human brain

Top: Specific tracer uptake in thalamus (large arrow) and cortical white matter (arrowhead) in a 67 years old male subject. Left=baseline study, right = blocking study. These punctate accumulations of tracer only appear in older subjects. Axial slices, level of thalamus. Bottom: Panel on left displays the relationship between age and total distribution volume (VT) in occipital cortex, fitted to a straight line with R=0.61 and $p<0.015$. The relationship of VT with age in cortical white matter (right panel) is best fit by a polynomial 2nd order equation, with R=0.59 and $p<0.05$. Occ=occipital cortex, wm=cortical white matter.